Noname manuscript No.
(will be inserted by the editor)

A variational approach to calculate the crack opening from a phase field description

Vahid Ziaei-Rad · Cheng Cheng · Yongxing Shen

Received: date / Accepted: date

Abstract Phase field methods for fracture are advantageous as they can predict crack nucleation and branching. However, the crack is not explicitly tackled. In some applications, it is required to detect the crack geometry. This paper deals with of the calculation of crack opening from typical phase field approaches. we provide a variational way, based on principle of virtual work, to calculate the crack opening from a phase field description, assuming that an explicit crack path is identified. Our approach is valid for any phase field description of a crack. Three sets of representative examples are provided to prove the performance of our method. An elastic solution is chosen as a benchmark to verify the calculation of crack opening.

Keywords Phase field method · Fracture mechanics · Crack opening

V. Ziaei-Rad
Laboratori de Càlcul Numèric, Universitat Politècnica de Catalunya (UPC BarcelonaTech), 08034 Barcelona, Spain
E-mail: vahid.ziaei@upc.edu

C. Cheng
800 Dongchuan Road, University of Michigan-Shanghai Jiao Tong University Joint Institute, Shanghai Jiao Tong University, Shanghai, 200240, China
E-mail: nole2010@sjtu.edu.cn

Y. Shen
800 Dongchuan Road, University of Michigan-Shanghai Jiao Tong University Joint Institute, Shanghai Jiao Tong University, Shanghai, 200240, China
E-mail: yongxing.shen@sjtu.edu.cn

1 Introduction

In this chapter, we aim to calculate the crack opening from a phase field approach to fracture. This can be considered as a second step for identifying the crack geometry, see Chapter **??** for the crack path identification.

The calculation of crack openings can be useful in some applications. One example is to estimate the durability of concrete structures. The cracks are more likely exposed to fluid or corrosive chemicals inside, hence, it is beneficial to investigate the openings [Pijaudier-Cabot et al(2009)Pijaudier-Cabot, Dufour, and Choinska].

Another example is hydraulic fracturing where the high pressure liquid inside the fracture causes further propagation. In most studies, the fluid pressure is obtained from a lower dimensional lubrication equation [Irzal et al(2013)Irzal, Remmers, Huyghe, and de Borst, **?**]. In order to solve the fracture flow from the lubrication equation, the crack openings need to be known.

One method was proposed by Dufour *et al.* [Dufour et al(2012)Dufour, Legrain, Pijaudier-Cabot, and Huerta] where the idea is to compare two effective non local strain: The one that controls damage and the other derived from a strong discontinuity analysis. The estimation was illustrated in a one-dimensional example close to failure.

In this chapter, we offer a variational approach to calculate the openings. The idea is to stabilize the effect of both the smeared crack and its equivalent explicit one by means of a virtual work equilibrium. Therein, phase field gradient is used as a weighted function to calculate the openings from displacement profiles $\boldsymbol{u}$. In Section 3, we provide three representative examples to test the performance of our method. Throughout this chapter, we frequently use the terminologies used in Chapter **??**

2 Approach to calculate the crack opening

In this section, we set up the problem of calculating the openings from phase field descriptions of crack. First, we introduce a variational formulation to replace the discrete definition of a jump set with a sufficient condition. Next, we present our variational approach which is based on the principle of virtual work. Finally, we discuss the special case of branched cracks where the method needs to be slightly modified to tackle the case.

2.1 The special case

Consider $\Omega = \mathbb{R}^2$. Let $\Gamma \subset \mathbb{R}^2$ be an identified crack path for $d(\boldsymbol{x}) = \exp\left(-\frac{|y|}{\ell}\right)$. Also, let $\boldsymbol{u}_y = u\boldsymbol{e}_y$ be such that $\boldsymbol{u}_y(y) \to \boldsymbol{u}^{\pm}$ when $y \to \pm\infty$, see Section **??**. Now, we define H_ℓ, as the openings, by a variational formulation:

$$H_\ell[\boldsymbol{u}, d] := \lim_{\ell \to 0} \int_{-\infty}^{\infty} -\boldsymbol{u}_y \frac{\partial d}{\partial y}\, dy = \boldsymbol{u}^+ - \boldsymbol{u}^-, \tag{1}$$

One sufficient condition for (1) is as below:

$$\lim_{\ell \to 0} \int_{0}^{\infty} \left(\left(\boldsymbol{u}^+ - \boldsymbol{u}^-\right) - \left(\boldsymbol{u}_y(y) - \boldsymbol{u}_y(-y)\right)\right) \frac{\partial d}{\partial y}\, dy = 0. \tag{2}$$

2.2 Variational formulation

With respect to (1), we present a general approach to calculate the openings from any phase field topology. Let $(\boldsymbol{u}, d)$ be a solution of (**??**), or an approximation to it. We equivalently identify $(\boldsymbol{u}, \Gamma)$ as an approximation of (**??**). Readers are referred to Chapter **??** for more explanations.

The main body of the approach is as follows: Let be δP a virtual pressure. We take virtual work by δP on the identified crack (Γ) be equal to the one on the smeared crack (d). Therefore, the following variational equality takes place:

$$\int_{\Gamma} \delta P(s) \cdot H(s)\, ds = -\int_{\Omega_0} \left(\delta P \circ \gamma^{-1} \circ \pi(\boldsymbol{x})\right) \left((\boldsymbol{u} - \boldsymbol{u}_{ref}) \cdot \nabla d\right)\, d\Omega, \tag{3}$$

where $\pi : \Omega \to \Gamma$ is the closest point projection, and $\boldsymbol{u}_{ref}$ is the rigid body motion of the sample. This term can be computed as below.

$$\boldsymbol{u}_{ref} = \frac{1}{|\Omega_0|} \int_{\Omega_0} \boldsymbol{u}\, d\Omega. \tag{4}$$

Note that in (3), $\pi(\boldsymbol{x})$ is the closest point projection of $\boldsymbol{x}$ on Γ, and $\boldsymbol{\gamma} : [s_1, s_N] \to \mathbb{R}^2$ is defined as a map, see Chapter **??**.

2.3 Numerical discretization

In this section, we adopt standard procedures to obtain Galerkin approximation for the problem in hand. We discretize the domain Ω with a mesh family $\{\mathscr{T}_h\}$, each member characterized by the mesh size h. We approximate δP and H merely on Γ with the standard first-order finite element basis functions associated with the knots ($k \in K$). Note that since the virtual pressure is free to choose, we merely use the basis functions to approximate it. See below:

$$H(s) = \sum_{i \in K} H_i N_i(s), \tag{5a}$$

$$\delta P(s) = \sum_{i \in K} \delta P_i N_i(s). \tag{5b}$$

Standard Galerkin approximations yield the following matrix form for (3):

$$\mathbf{MH} = \mathbf{F}, \tag{6}$$

where $\mathbf{H} = \{H_P\}$ is a vector that contains the nodal degrees of freedom for H. The explicit expressions of the matrices involved in (6) read:

$$\sum_{j \in K} \left(\int_{\Gamma} N_i(s) N_j(s) H_j \, ds \right) = - \int_{\Omega} \left(N_i \circ \gamma^{-1} \circ \pi(\boldsymbol{x}) \right) \left((\boldsymbol{u} - \boldsymbol{u}_{ref}) \cdot \nabla d \right) \, d\Omega. \tag{7}$$

2.4 The case of branching

In general, the method work for any smeared representative of a crack. However, from our experience, this way sometimes may not be accurate for the case of a branched crack, as the phase field topology is too smooth near the junctions. Hence, for the sake of accuracy, we modified the phase field topology and the region of integration in (3).

We proceed as follows: Let j be a junction and aj be a simple identified branch for a given phase field, see Figure 5. For aj, first we identify the region $\Omega_{aj} \subset \Omega$, which is the set of all points in Ω closer to aj than other branches, and in order to calculate the openings at aj, we take Ω_{aj} for (3) as the region integration in place of Ω. Second, we replace the current topology of the phase field by that of the *equivalent phase field* of aj.

Moreover, we slightly modify the phase field profile as follows: For point j we virtually extend aj along the same direction to $j\prime$, one knot spacing apart from j. Hence, the new branch is $ajj\prime$. And, we consider the equivalent phase field for $ajj\prime$ as the one to be incorporated in (3). This way will also prevent the high gradient phase field at j, now will be like a crack tip, to unstabilize the results. The results, shown in Section 3.2, prove that the current way leads to an opening profile aligned with that of the chosen benchmark.

3 Numerical examples

In this section, we present three representative sets of numerical examples to demonstrate the performance of our variational approach. The examples consist of a curved crack, a branched crack, and multiple cracks.

In this section, we investigate a square plate with some initial cracks. Two geometric setups are depicted in Figure 1. For the simple curved case and the branched case, the specimen is under a direct tension test in which a displacement with magnitude $\boldsymbol{u}_D$ is imposed on the top and bottom edges (Figure **??**) while for the case of multiple cracks, the loading is imposed on all edges (Figure **??**).

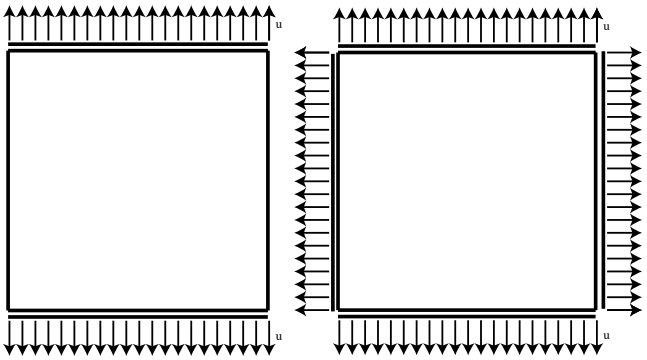

Fig. 1: Schematic of a cracked square plate under a single-edge-notched tension test. A uniform displacement loading $\|u_D\|$ normal to the edges is applied on (a) top and bottom edges for the cases in 3.1 and 3.2, (b) on the whole edges for the case of Section 3.3. Also, some initial crack is assumed for each set of examples.

Throughout this section, in order to solve for (**??**), we will adopt the values of the parameters given in Table 1, unless otherwise noted.

Table 1: Default parameter values for the examples

Name	Symbol	Value
Lamé constant	λ	120GPa
Shear modulus	μ	80GPa
Critical energy release rate	g_c	2.7×10^{-3}kN/mm
length scale ratio	h/ℓ	0.2
Boundary displacement	u_D	10^{-3}mm

To better evaluate our results, we will follow this procedure to obtain the displacement $\boldsymbol{u}$ field and the phase field d as input for all examples: We first assume a crack path, either Γ or Γ^*, see Chapter **??**. Afterwards, we obtain the equivalent phase field d_{Γ^*} from (9). With that, we identify the bounding element set E to d_{Γ^*}. Next, with the mesh $\mathscr{T}_h$, we minimize (**??**) with the nodal values of d_{Γ^*} in Ω_E. We impose boundary displacement $\boldsymbol{u} = \boldsymbol{u}_D$ so that a tension test be modeled. The approximation is then taken as input for the subsequent examples.

Let $\boldsymbol{u}^*$ be the minimizer of $\Pi(\cdot, \Gamma^*)$ with the constraint $\boldsymbol{u}^* = \boldsymbol{u}_D$ on $\partial\Omega_D$, where Π is defined in (**??**). We take $\boldsymbol{u}^*$ as a benchmark to evaluate our calculation of the crack opening from the approximation of (**??**) for the subsequent examples. Let $\boldsymbol{u}$ be obtained from an approximation of (**??**). In order to justify our benchmark, we define ε as (8):

$$\varepsilon := \frac{\|\boldsymbol{u} - \boldsymbol{u}^*\|_{L_2(\Omega)}}{\|\boldsymbol{u}^*\|_{L_2(\Omega)}}, \tag{8}$$

An advantage of setting the phase field input d as above is that Γ^* is used in a consistent way for the calculation of both $\boldsymbol{u}$ and $\boldsymbol{u}^*$.

3.1 Simple curved crack

This example is chosen to prove that the algorithm is capable of calculating the openings with a considerable curvature, see Figure 2. Here in separate snapshots the element set E, and the output from the crack detection algorithm Γ, and the assumed crack path Γ^* are shown. In this example, Γ^* is taken as the cubic spline passing through the points $(0.3, 0.5)$, $(0.5, 0.2)$, and $(0.7, 0.5)$ with appropriate end conditions following [Rangarajan et al(2015)Rangarajan, Chiaramonte, Hunsweck, Shen, and Lew].

Figure 3 plots the crack opening by $\boldsymbol{u}$, labeled as *variational approach* and $\boldsymbol{u}^*$ as *benchmark*.

3.2 Branched crack

In this example, we consider a phase field d associated to a branched crack, see Figure 4. This crack consists of three straight segments with the junction at $j = (0.5, 0.5)$, and the three crack tips at $a = (0.3, 0.5)$, $b = (0.7, 0.7)$, and $c = (0.7, 0.3)$.

Figure 5 depicts the openings of the three segments for a set of knots spacing $2h$. Also shown is the openings for the benchmark. Readers are referred to 2.4 for further explanations about the special issues for the case of branching.

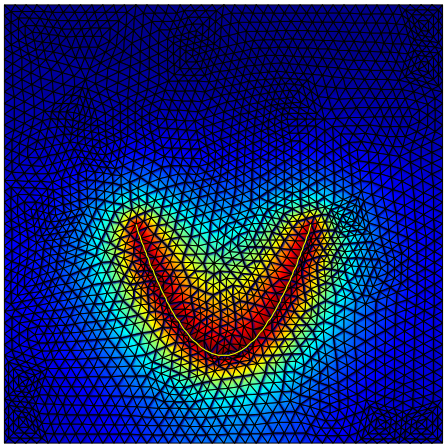

Fig. 2: A simple curved crack. Phase field topology, and Γ^*, the "exact solution" in yellow, are shown. There is a conforming mesh to Γ^*.

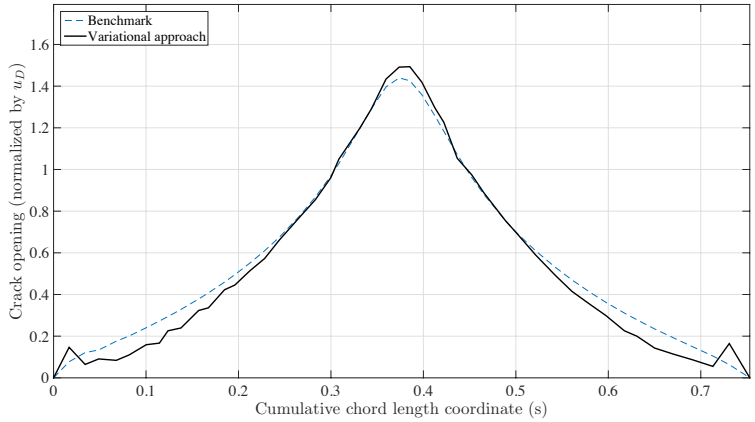

Fig. 3: A simple curved crack. A comparison of opening by $\boldsymbol{u}$ and $\boldsymbol{u}^*$ is made. Good agreement is observed. $\boldsymbol{u}_{ref}$ is calculated by (4).

3.3 Multiple cracks

In this example, we calculate the opening for two non-intersecting cracks with a certain distance. Phase field topology is shown with Γ and Γ^*, see Figure 6.

Figure 7 illustrates the openings for the horizontal (left) and vertical crack (right), compared to ω^*. Three sets of knots are shown for each segment. It can be seen that the ones with smaller knot spacings tends more to the benchmark.

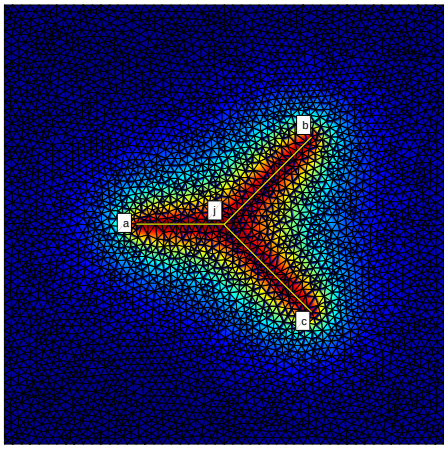

Fig. 4: A branched crack. Phase field diagram and Γ^*, the "exact solution" in yellow, are shown. There is a conforming mesh to Γ^*. We labeled the junction and the three crack tips.

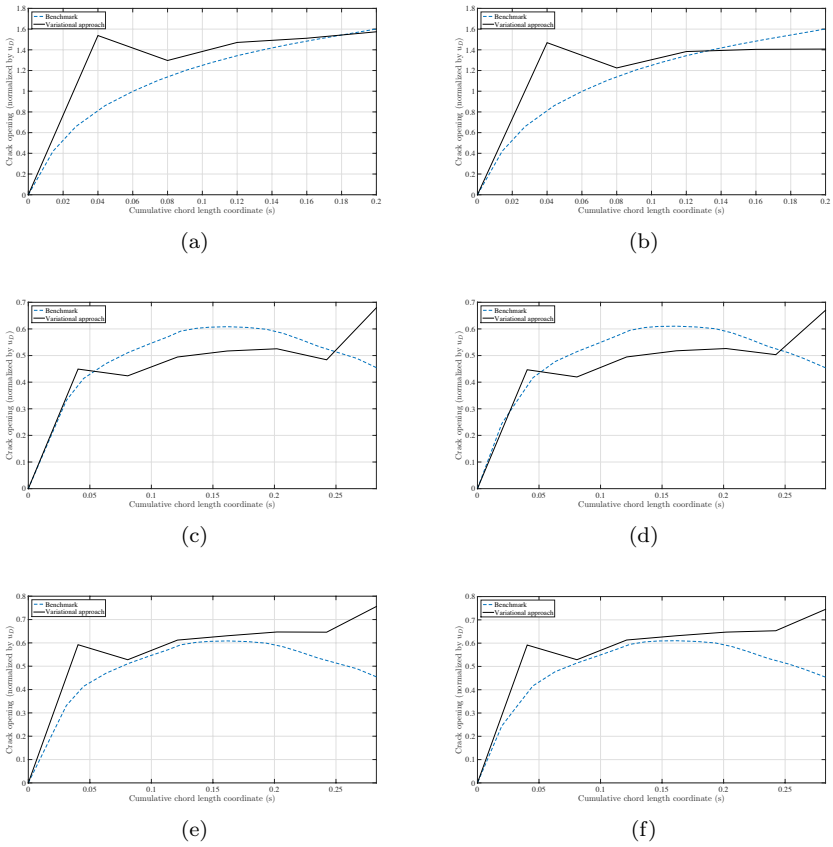

Fig. 5: A branched crack. The openings for the segments aj, bj, and cj are subsequently shown in (left) for model B, and (right) for model C. Curves in blue are for the benchmark.

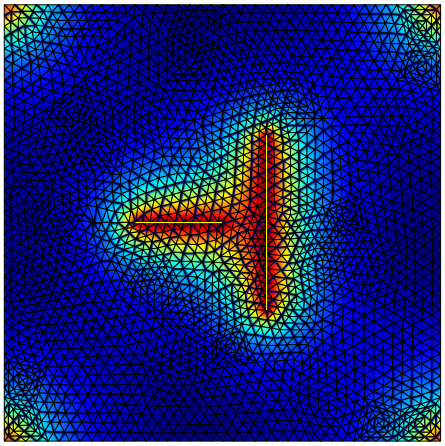

Fig. 6: Multiple cracks. Phase field diagram and Γ^*, the "exact solution" in yellow, are shown. There is a conforming mesh to Γ^*.

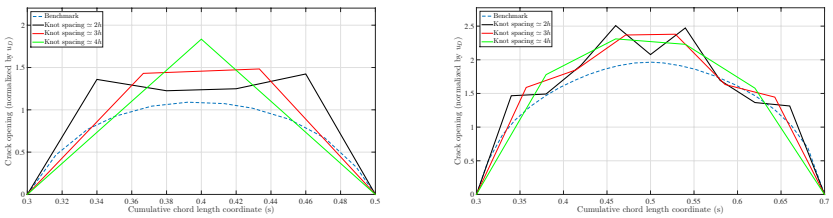

(a) (b)

Fig. 7: Multiple cracks. The openings along the horizontal and vertical cracks are shown in (a) and (b), accordingly. Also shown is ω^* in blue dashed lines. The results are presented for three sets of knots with different knot spacings for each segment.

A Crack identification

This section devotes to setting up the problem of tackling the crack from a phase field description. We introduce a variational way to identify a set of discontinuities ($\Gamma \subset \Omega$) from a phase field solution of (**??**), or an approximation to it ($\boldsymbol{u}, d$).

Let $\boldsymbol{x} = (x, y)$ be a generic point in $\Omega = \mathbb{R}^2$. Minimizing (**??**) while $\boldsymbol{u} = 0$, under the assumptions that $d(y = 0) = 1$ and $\partial d/\partial y \to 0$ as $y \to \pm\infty$ leads to following phase field functional for any x:

$$d(\boldsymbol{x}) = \exp(-|y|/\ell). \tag{9}$$

This corresponds to a phase field diagram at $x = \text{const.}$ for an infinite horizontal crack ($y = 0$).

We define $d_\Gamma : \Omega \to [0, 1]$ as the equivalent phase field for Γ. With respect to (9), analogically we propose the following functional to determine the equivalent phase field, d_Γ:

$$d_\Gamma(\boldsymbol{x}) = \exp(-\rho(\boldsymbol{x}, \Gamma)/\ell), \tag{10}$$

where $\rho(\boldsymbol{x}, \Gamma)$ is the minimum distance from $\boldsymbol{x}$ to Γ.

We aim to develop a consistent method to extract $\Gamma \subset \Omega$ whose equivalent phase field d_Γ, as defined in (10), fits nicely to d in Ω. Note that ideally we try to find a Γ that makes d_Γ and d be equal.

Now, the crack identification problem reads: Among all curves, find Γ that minimizes N_d:

$$N_d[\Gamma] := \|d - d_\Gamma\|^2. \tag{11}$$

As it is difficult to search among all possible curves, we limit ourselves to the a class of cubic splines contained in Ω in order to render the problem with finite dimensions.

Acknowledgements This work is supported by the National Natural Science Foundation of China, grant # 11402146. Y. S. acknowledges the support of the Young 1000 Talent Program of China.

References

[Dufour et al(2012)Dufour, Legrain, Pijaudier-Cabot, and Huerta] Dufour F, Legrain G, Pijaudier-Cabot G, Huerta A (2012) Estimation of crack opening from a two-dimensional continuum-based finite element computation. International Journal for Numerical and Analytical Methods in Geomechanics 36(16):1813–1830

[Irzal et al(2013)Irzal, Remmers, Huyghe, and de Borst] Irzal F, Remmers J, Huyghe JM, de Borst R (2013) A large deformation formulation for fluid flow in a progressively fracturing porous material. Computer Methods in Applied Mechanics and Engineering 256:29 – 37

[Pijaudier-Cabot et al(2009)Pijaudier-Cabot, Dufour, and Choinska] Pijaudier-Cabot G, Dufour F, Choinska M (2009) Permeability due to the increase of damage in concrete: From diffuse to localized damage distributions. Journal of Engineering Mechanics 135(9):1022–1028

[Rangarajan et al(2015)Rangarajan, Chiaramonte, Hunsweck, Shen, and Lew] Rangarajan R, Chiaramonte MM, Hunsweck MJ, Shen Y, Lew AJ (2015) Simulating curvilinear crack propagation in two dimensions with universal meshes. International Journal for Numerical Methods in Engineering 102(3–4):632–670